ADVANCES IN MATERIALS SCIENCE, Vol. 18, No. 2 (56), June 2018

DOI: 10.1515/adms-2017-0030

N. Zienkiewicz, J. Paradowska, W. Serbiński, G. Gajowiec, A. Hernik, A. Zieliński

Gdansk University of Technology, Faculty of Mechanical Engineering, Department of Materials Science and Welding Engineering, 11/12 Narutowicza, 80-233 Gdańsk, Poland
azielins@pg.edu.pl

OXIDATION AND HYDROGEN BEHAVIUR IN Zr-2Mn ALLOY

ABSTRACT

The purpose of the present research was to determine the oxidation and hydrogenation behavior in the new Zr-2Mn alloy. The oxidation of alloy was performed at temperatures between 350°C and 900°C for 30 minutes. The hydrogen charging was made for 72 h at a current density 80 mA/cm^2. The charged samples were heat treated at 400°C for 4 h to obtain a uniform hydrogen profile content across the sample. The oxidation resulted in an appearance of non-uniform oxide layers of thickness increasing with temperature. The surface damage was observed at higher temperatures 700 and 900°C. After charging with hydrogen followed by annealing no hydrides were found. The observed effect is evidence that the oxide layers may form effective barriers against hydrogen diffusion even if they are partially degraded. The absence of hydrides or hydride cracking may be caused by an absence in Zr-Mn alloys of such phase precipitates, which may trap diffusive hydrogen and initiate the hydrides. The positive influence of manganese on the formation of the thick oxide layer and relative resistance to delayed hydride cracking may be attributed to its affinity of oxygen, the ability to form thick and compact oxide layers during oxidation, the formation of solid solution in zirconium and no precipitates enhancing nucleation of hydrides.

Keywords: *zirconium alloys, nuclear reactor materials, oxidation, hydrogen embrittlement*

INTRODUCTION

Zirconium alloys have been applied in the nuclear industry for many years, mainly as nuclear fuel cladding tubes and pressure tubes because of their low neutron absorption, good strength and corrosion resistance at high temperatures [1]. The fuel claddings are exposed to very serious risks, in particular in nuclear accidents to temperatures 1000°C and more, high tensile stresses and the possible presence of oxygen and hydrogen. Hydrogen is produced as a result of aqueous corrosion of Zircaloy claddings [2] or cooling water decomposition in LOCA (*loss-of-coolant accident*) [3]. Hydrogen may diffuse into the core material and, when its solubility exceeds the terminal limit, it can precipitate in hydride form. Such behavior is usually supposed to initiate the hydride-enhanced degradation. However, such phenomenon

occurs at high hydrogen amounts and much less has been investigated as to what may happen at low and intermediate hydrogen contents.

When the Zr alloys are subjected to elevated temperatures, the zirconium oxides are formed. Such oxide layers may likely form in some conditions the effective barrier against hydrogen entry and be permeable in another. On the other hand, the oxidation at high temperatures may result in thick and cracked oxide layers, causing so-called breakaway oxidation followed by descaling of the oxide layers. This phenomenon is presumably caused by either different volume expansion coefficients of substrate and oxide phase, by the presence of two oxide zones of the different crystalline structure after allotropic transformation, or by oxide porosity [4]. The breakaway oxidation usually starts at about 950-1200°C after a certain initiation time ranging from 2 to 12 ks. There is no clear whether the oxide layer formed at a temperature of the breakaway phenomenon may be still efficient against hydrogen entry and what is the effect of descaling on the hydrogen absorption. Moreover, the oxide phase transformation and descaling may appear at a lower temperature and in a shorter time, comparing to those shown above, in the presence of high stresses [5].

The hydrogen absorption is related to the hydrogen pressure, exposure time and temperature, and the effects much less investigated for Zr alloys, to the material composition and structure. Nb reduced hydrogen pickup fraction whereas Cu increased it. The alloy with coarser $Zr(Fe, Cr)_2$ precipitates exhibited a lower hydrogen pickup fraction than the alloy with finer precipitates [6]. At the moderate and high hydrogen contents, hydrogen uptake evolved linearly with the time that could be attributed to the formation of a hydride layer of constant thickness moving along the sample at a velocity of about 100 mm/min [7]. The precipitation of Fe, Cr and Ni affected the process activation energy estimated at 54 kJ/mol. Even in the presence of hydrides, dislocations can enhance precipitation of the hydrides [8].

An important problem to recognize is the mechanism by which hydrogen enters zirconium alloys through the oxide layers. Cox [9] claimed that was no evidence to justify the assumption that this hydrogen would migrate through the ZrO_2 lattice or crystallite boundaries, and that the hydrogen uptake would occur only locally. On the contrary, a relatively uniform hydrogen diffusion process through the oxide was discussed [10]. The hydrogen diffusion rate in the oxide layer increased with increasing Nb amount, in particular for thicker layers [11]. The oxides present on zirconium alloys were more permeable to deuterium than those on pure zirconium. Finally, the existence of the O–H bonds within the oxide layer was said to decrease the hydrogen diffusion [12]. The hydrogen solubility in the ZrO_2 oxide was estimated from the thermal desorption spectra to range from 10^{-5} to 10^{-4} mol H/mol oxide and to decrease with increasing temperature [13]. The oxide layer was recognized as the hydrogen diffusion barrier, but there are no data on how effectively the structure and thickness of oxide layer would affect the hydrogen entry into the metal.

The equilibrium between the interstitial hydrogen and hydride phase in bulk material was described several times. The terminal hydrogen solubility in zirconium was found as about 80 mass ppm at 300°C and 200 mass ppm at 400°C [14]. The hydrogen solubility in β-Zr was 7-9 times higher than in α-Zr within the temperature range 247-300 °C [15]. The interstitial hydrogen may be bound by some traps. The regions of high dislocation density represent such strong traps for hydrogen [16].

The hydrides were very extensively studied. The hydride precipitation and dissolution enthalpies were estimated at 24 kJ/mol H and 32.5 kJ/mol H, respectively [17]. The enthalpies of dissolution and precipitation of hydrides in the Zircaloy-2 pressure tube material were 30.0–34.5 and 25.9–26.3 kJ/mol, and in Zr–2.5Nb pressure tube alloy 34.5 and 17.2–22.8 kJ/mol, respectively [18]. Even if hydride could appear at high temperatures because of increasing diffusion and absorption, the hydride phase after in situ (gas) or ex-situ (cathodic) exposure of the Zr surface to hydrogen was observed already at 20°C [19]. The hydride phase

on the surface subsequently decomposed with temperatures increasing to 600°C. The Zr–Sn–Fe–Nb tubes electrolytically charged with hydrogen revealed that the hydrides were mostly circumferentially oriented and identified as e-ZrH_2 and γ-ZrH phases [20].

As can be seen, commercial zirconium alloys for fuel pellets are either Zr-Sn or Zr-Nb alloys. The purpose of this research was to investigate the oxidation and hydrogen charging of oxidized new Zr-2Mn alloy compared to the behavior of two other alloys, Zr-Sn and Zr-Hf. So far, there has been no research, and such studies are important for further development of zirconium alloys.

EXPERIMENTAL

The Zr-2Mn alloy was obtained by melting the Zr and 2 wt.pct. Mn powders in an electric oven at the temperature of 1880°C in vacuum 0.05 mbar for 90 min. The thoroughly mixed powders were put into graphite melting and heated for 200 min. The cooling was conducted in the oven. The test specimens of dimensions 20x20x50 mm were cut from the ingot and polished with SiC abrasive papers, No. 2000 as the last, and diamond paste of 3 μm grit size, then cleaned with distilled water in an ultrasonic bath and dried in warm air.

All specimens were oxidized in the electric oven for 30 min. in the air at a temperature ranging between 350 and 900°C and then electrolytically charged with hydrogen; the tested specimen was a cathode, and Pt grid was an anode. The cathodic charging was performed at room temperature for 72 h at the voltage 2.6 V. Such voltage value resulted for reference no-oxidized specimen at current density 80 mA/cm^2. For oxidized specimens, the values of resultant current were lower (see Results). The hydrogen charged specimens were cleaned with water, dried in warm air and heat treated for 4 h at 400°C to obtain the uniform hydrogen profile across the sample.

The microscopic examinations of the specimens were performed with the JEOL 7800 F scanning electron microscope, equipped with EDS/EDAX (Cambridge Instruments), on the cross-sections of polished specimens before any test (reference samples), after the oxidation and after the hydrogen charging. The etching of cross-sections was made with the solution containing 45 cm^3 of 65% HNO_3, 10 cm^3 of 40% HF and 45 cm^3 of distilled water.

RESULTS

Microstructure of as-fabricated alloy

The samples of the microstructure are shown in Fig. 1. The dendritic structure was developed. The presence of two phases, the matrix and eutectoid are observed. Fig. 2 shows the examples of surfaces of the obtained alloy. Fig. 2a demonstrates the areas of subsequent EDS examinations.

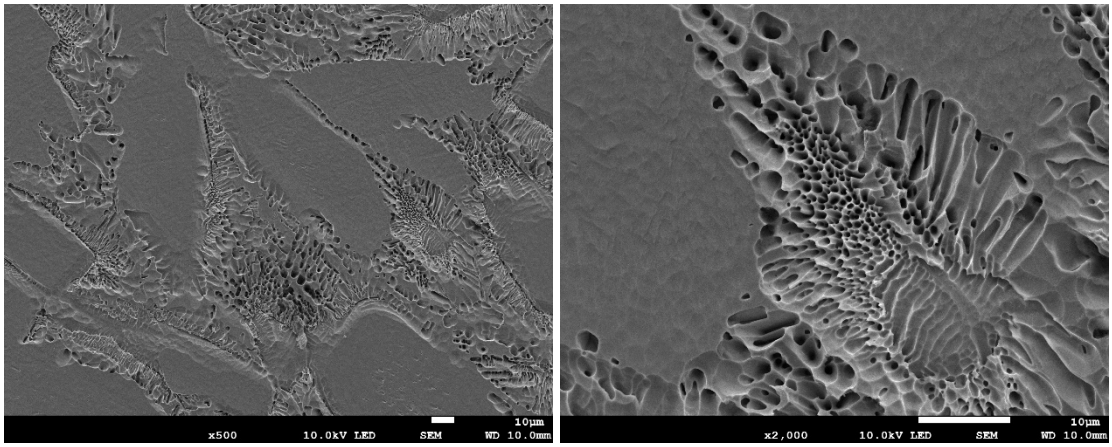

Fig. 1. The cross-sections of as-fabricated Zr-2Mn alloy

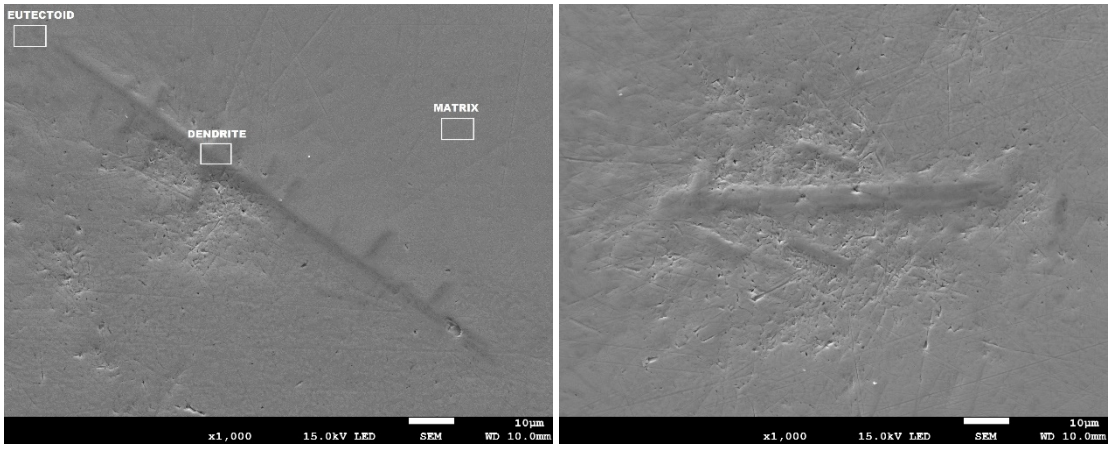

Fig. 2. The surfaces of as-fabricated Zr-2Mn alloy with indicated (on left image) areas of EDS examinations

Chemical composition

The chemical composition was measured by EDS/EDAX equipment (Gdansk University of Technology, Nanotechnology Center B) in three different areas: inside some dendrites, in the eutectoid area, and the matrix. The dendrites were significantly enriched with manganese at the expense of zirconium. Table 1 illustrates the means of three independent measurements, for each area (Figs. 3-5 – examples of the EDS examinations). The examinations were made in areas shown in Fig. 2.

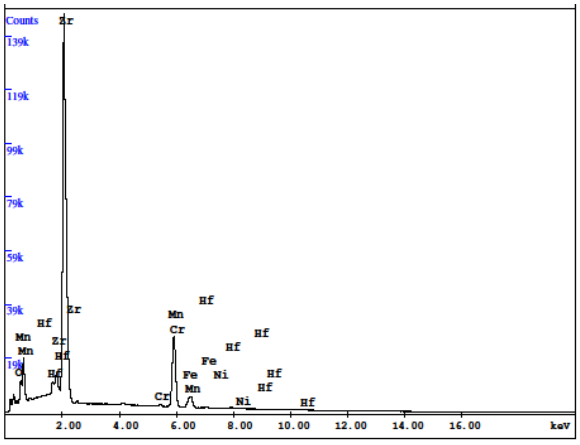

Fig. 3. EDS spectrum and results for dendritic area

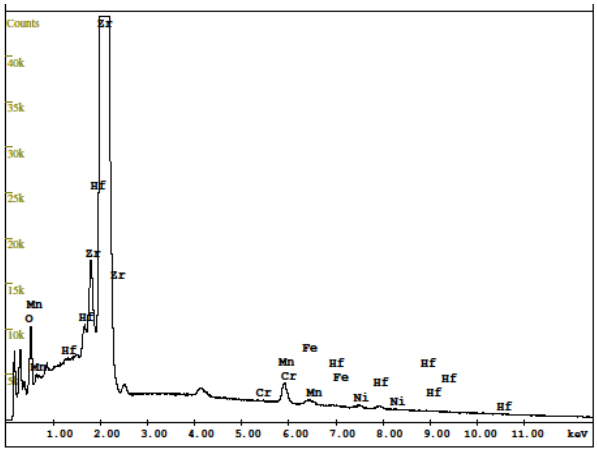

Fig. 4. EDS spectrum and results for eutectoid area

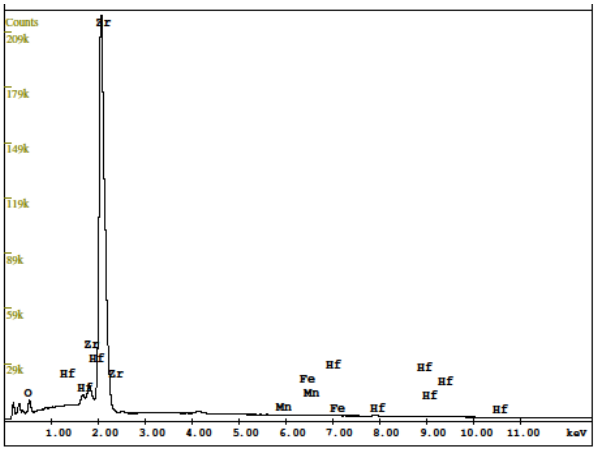

Fig. 5. EDS spectrum and results for matrix area

Table 1. *Chemical composition of Zr-2Mn alloy in different area, wt. %*

Element	Dendritic structure	Eutectoid	Matrix
O	4.56	5.85	5.95
Zr	64.57	85.04	89.56
Cr	0.65	0.22	0.06
Mn	24.19	4.55	0.27
Fe	1.88	0.66	0.28
Ni	0.20	0.19	0
Hf	3.95	3.49	3.88

Oxidized surfaces

The Zr-Mn alloy (Figs. 6-8) showed the dendritic structure consisting of a solid solution of manganese in zirconium and eutectics composed of this solid solution and intermetallic phase Mn_2Zr as suggested by phase diagram.

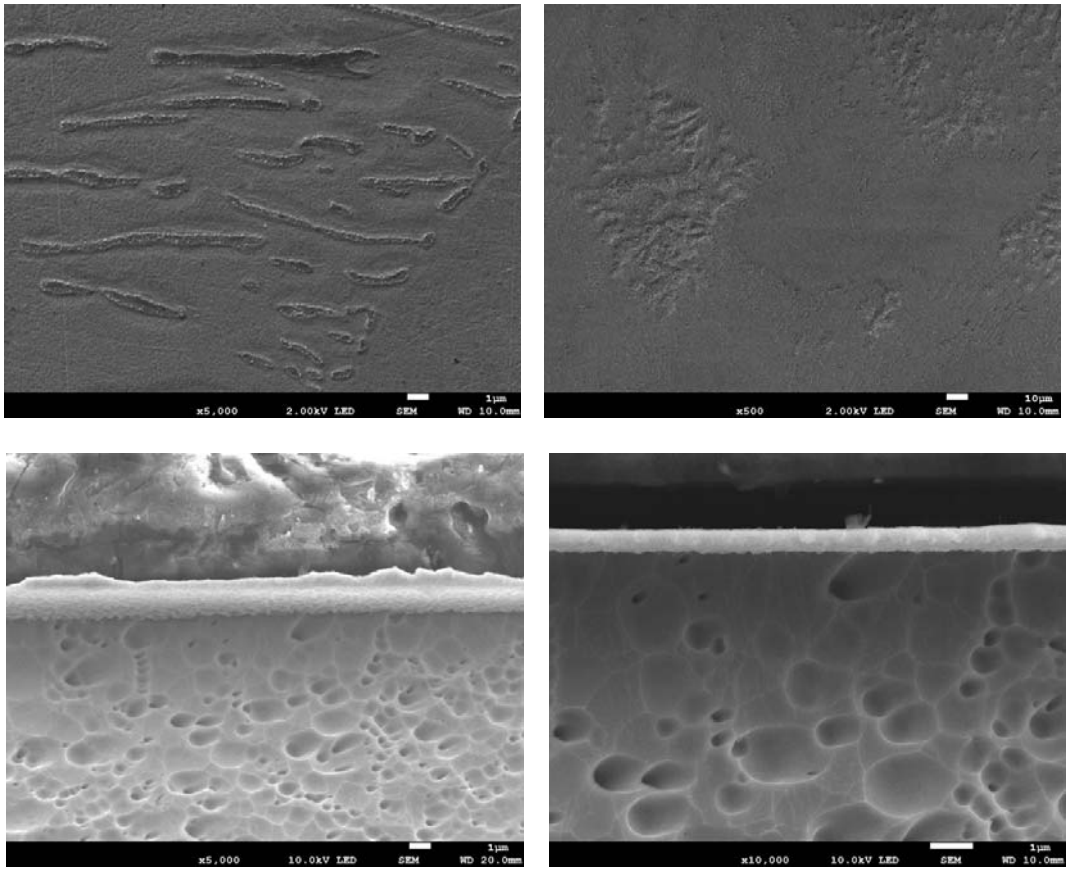

Fig. 6. Surfaces (top) and cross-sections (bottom) of Zr-Mn2 alloy oxidized at 350°C

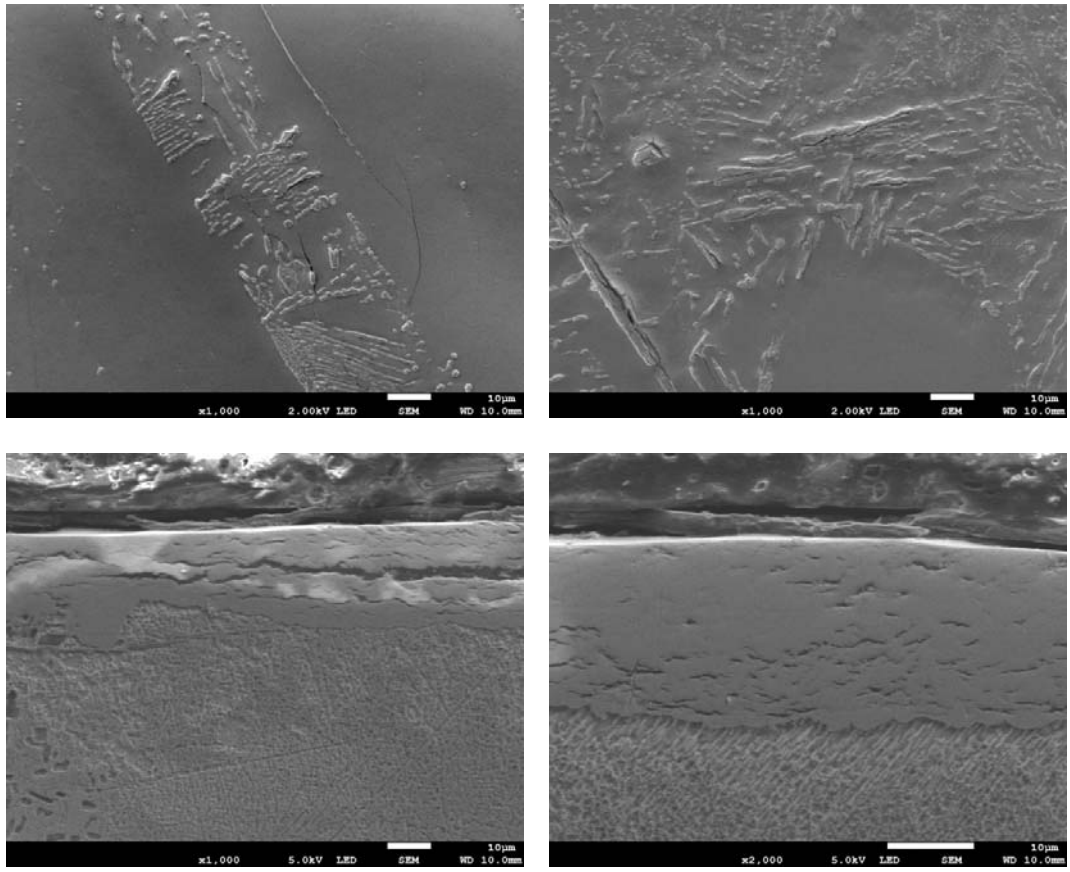

Fig. 7. Surfaces (top) and cross-sections (bottom) of Zr-Mn2 alloy oxidized at 700°C

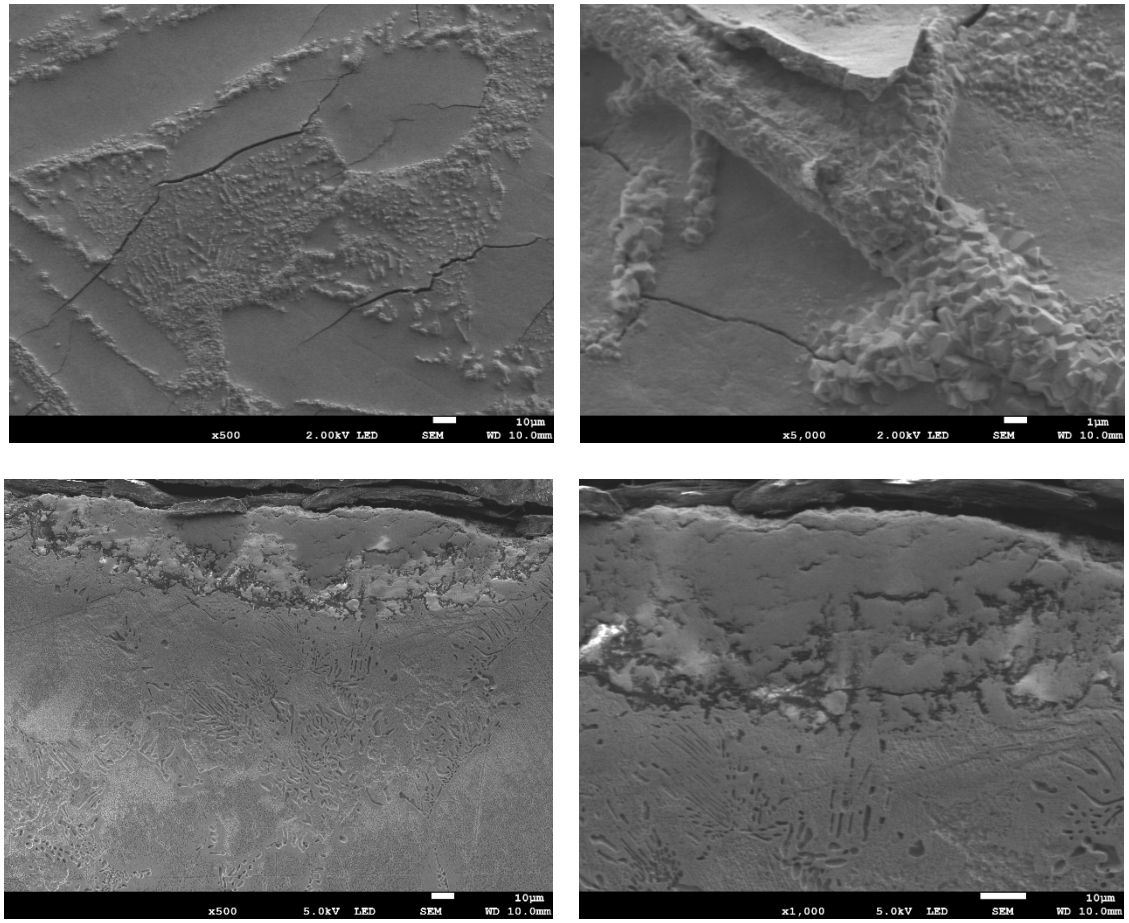

Fig. 8. Surfaces (top) and cross-sections (bottom) of Zr-Mn2 alloy oxidized at 900°C

After oxidation at temperature 350°C, the layer approaching 1 μm in thickness was observed. The oxide layer formed on Zr-Mn alloys after oxidation at higher temperatures were thicker, cracked and highly defragmented in case of 900°C oxidizing.

Hydrogen charging of non-oxidized and oxidized Zr-2Mn alloy

The cross-sections of oxidized at a different temperature, hydrogen charged and annealed at 400°C specimens are shown in Figs. 9-12. Neither hydrides nor cracks were found for any oxidation temperature or non-oxidized alloy.

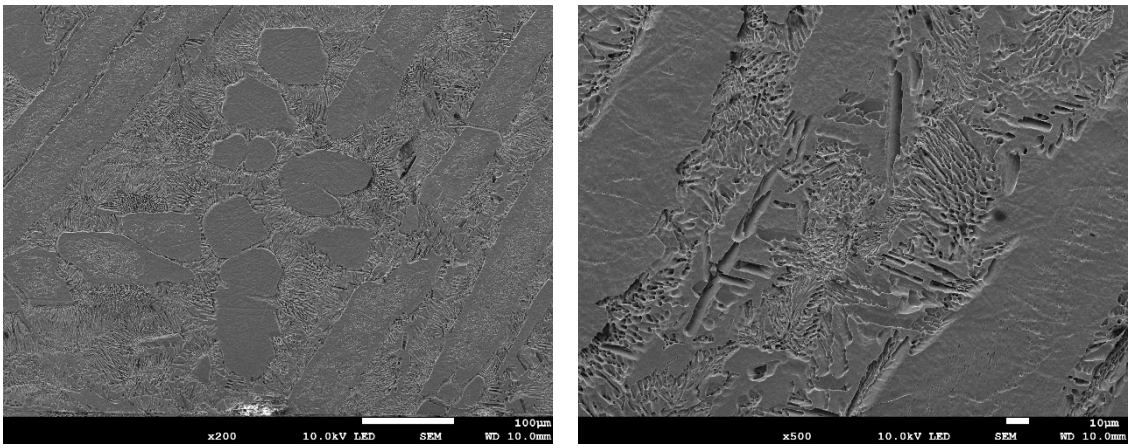

Fig. 9. Cross-sections of non-oxidized Zr-Mn2 alloy, hydrogen charged and annealed at 400°C

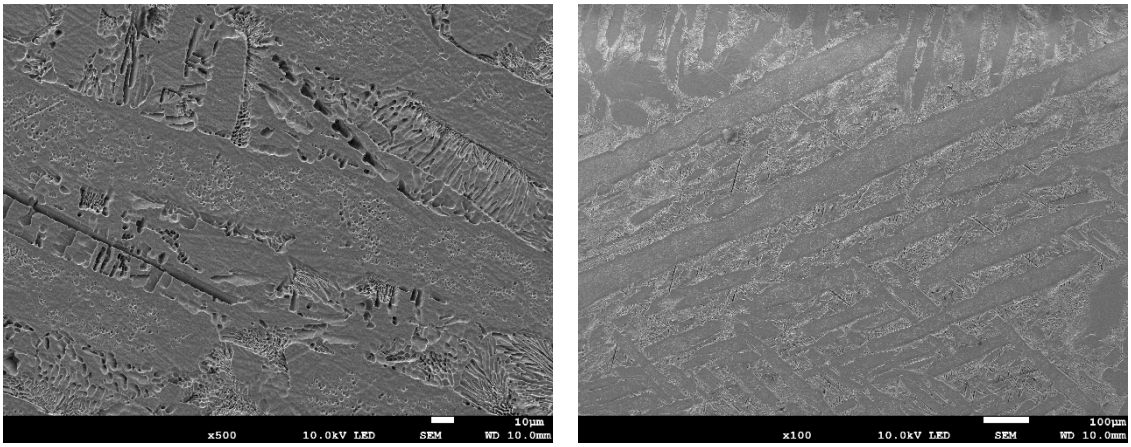

Fig. 10. Cross-sections of Zr-Mn2 alloy oxidized at 350°C, hydrogen charged and annealed at 400°C

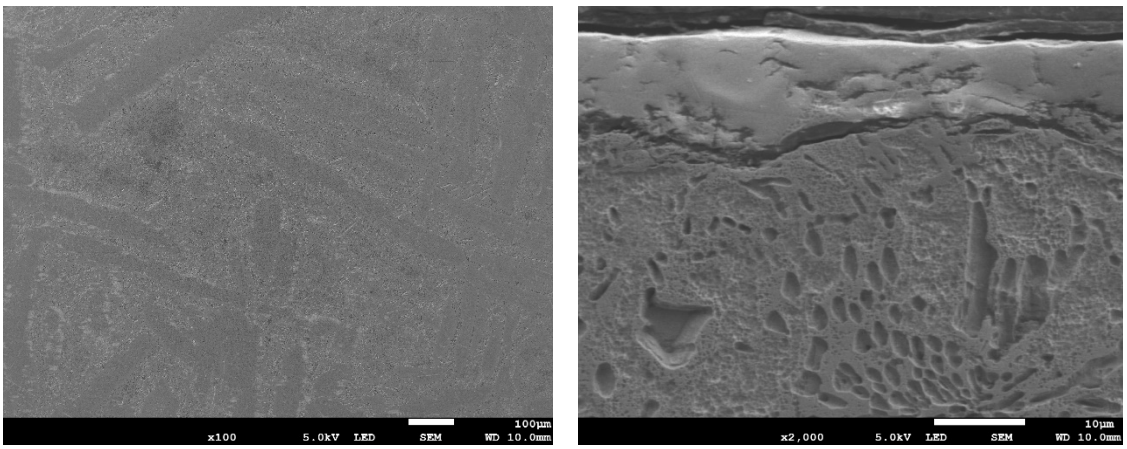

Fig. 11. Cross-sections of Zr-Mn2 alloy oxidized at 700°C, hydrogen charged and annealed at 400°C

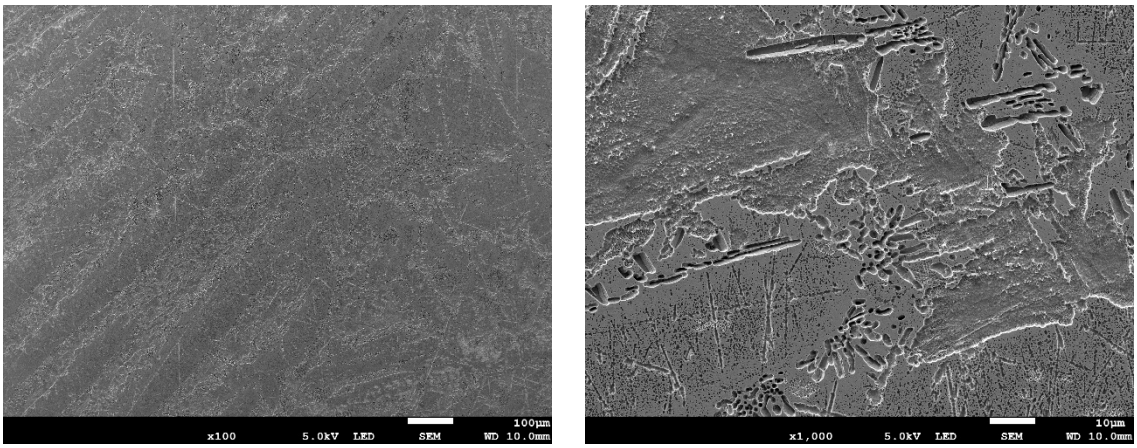

Fig. 12. Cross-sections of Zr-Mn2 alloy oxidized at 900°C, hydrogen charged and annealed at 400°C

Time – voltage relations

For both alloys non-oxidized or oxidized at 350°C, after adjusting the voltage about 2.65 V, the resultant current density 80 mA/cm^2 was constant during the whole test duration. For two other oxidation temperatures, 700 and 900°C, the voltage necessary to keep the constant current was about 6-8 V and after some hours started to decrease and at the end of the test was about 2.65 V.

DISCUSSION

Effect of oxidation temperature on an appearance and features of oxide layers

The effect of chemical composition on the oxidation behavior is undeniable and significant. It is known that unalloyed zirconium forms white porous oxide films, and Zr-Sn (zircaloys) alloys – dark tightly adherent oxide layers [3]. However, all oxide layers are substantially partly damaged after oxidation at 700°C and, to a greater extent, 900°C. The effects of both oxidation temperature and time on the appearance of oxide layers on some zirconium alloys were already extensively investigated [21]. This research proved again the gradual oxidation of all tested alloys resulting in increasing layer thickness. What is new here, is the degradation of oxide layers already at 700°C, similar to our previous work on Zr-Hf and Zr-Sn alloys, well below breakaway oxidation temperatures thus far reported, being proof of an important role of thermal stresses in the initiation of cracking, likely in the area of triple grain boundaries. The experiments were designed to obtain such stresses due to oxidation and fast removal of specimens from the oven to the air.

Effect of oxide layer on hydrogen absorption and degradation

The applied cathodic charging has been already used several times [22-26] and may result in the hydrogenation of Zr alloys even at room temperature after further annealing. The hydrogen content in these tests was not measured, but it should be close to the values given for similar alloys in our earlier research [27]. Such hydrogen content is certainly above the limit hydrogen solubility value at room temperature. So far, it is not evidence of hydrogen absorption by Zr-Mn alloys. It seems that is similar for pure zirconium and its alloys for nuclear applications.

The effect of an oxide layer on hydrogen absorption is crucial. In all previous research and this one, very thin oxide layers in all Zr alloys in as-received state or oxidized at 350°C (working conditions of fuel claddings) were found. However, in this investigation, the oxide layer is much thicker, likely thanks to the great affinity of oxygen to manganese. The permeation of hydrogen through present cracks and nanopores is possible even at room temperature as shown in our earlier work for Zircaloy-2 alloy. The degradation of oxide layer occurs by the breakaway effect and by its fracture by hydrogen of high fugacity.

The partial oxide layer degradation at high temperatures due to the breakaway effect might be followed by fast hydrogen absorption by a bare metal. In other words, when oxides are removed or are highly porous or cracked, the possibility for hydrogen to enter the bare metal might be similar to that of the as-received alloy. As previously here described, the barrier effect can appear either for highly damaged or porous oxide layer for some alloys and some oxidation temperatures. The oxide resistance to hydrogen entry related to the oxide thickness and continuity decreases for tested alloys in order: Zircaloy-2 > Zr-Mn > Zr 702. The reason for that is the influence of the alloying element on the structure of oxide layer (thickness is similar for all tested alloys), i.e., mainly presence of cracks and nanopores, their length and size, and so forth.

Effect of manganese on hydrogen behavior in the metal

The Zr-2Mn alloy revealed no hydrides without any its oxidation or after oxidation at any temperature. Such effect might be attributed to the barrier effect of the oxide layer, but

certainly, it is also the effect of an absence of micro hydrides. The hydrogen precipitation is possible also at low temperature as already observed [28].

The precipitation of hydrides at the same hydrogen charging conditions was observed in our earlier research for Zircaloy-2 and at low hydrogen content. It was attributed to the presence of $Zr(Fe, Cr)_2$ precipitates, which may form strong hydrogen traps. The Zr-rich phases containing such elements as Cu, Fe, Ni, Sn, Nb, and V create effective hydrogen traps in Zr alloys [29].The local high hydrogen content exceeds its terminal solubility, and the hydrides may appear, grow and decompose at such sites. Presumably, in Zr-Mn alloys, there are no such phase precipitates.

CONCLUSIONS

The oxidation of Zr-2Mn alloy is pronounced already after oxidation at 350°C, much lower than for Zr-Sn and Zr-Hf alloys, thanks to a great affinity of oxygen to manganese.

The degradation of oxide layers starts for Zr-2Mn alloy at 700°C, similar to that of another zirconium alloys, lower than expected because of thermal stresses.

The formation of hydrides initiating the delayed hydride cracking is not observed for Zr-Mn alloy, presumably because of an absence of phase precipitates being strong hydrogen traps.

ACKNOWLEDGMENTS

The authors gratefully acknowledge the technical assistance of Dr. Krzysztof Dudzik, Gdynia Maritime University, in preparation of the Zr-Mn cast alloy. The research was supported by the National Science Center, Poland, under the project entitled “Hydrogen degradation of oxidized zirconium alloys," No. 2013/11/B/ST8/04328.

REFERENCES

1. Bair J., Asle Zaeem M., Tonks M.: A review on hydride precipitation in zirconium alloys. J. Nucl. Mater. 466 (2015) 12–20.
2. Suman S., Khan M.K., Pathak M., Singh R.N., Chakravartty J.K.: Hydrogen in Zircaloy: Mechanism and its impacts. Intl. J. Hydrogen Energy 40 (2015) 5976–5994.
3. Zielinski A., Sobieszczyk S.: Hydrogen-enhanced degradation and oxide effects in zirconium alloys for nuclear applications. Intl. J. Hydrogen Energy 36 (2011) 8619–8629.
4. Baek J.H., Jeong Y.H.: Breakaway phenomenon of Zr-based alloys during a high-temperature oxidation. J. Nucl. Mater. 372 (2008) 152–159.
5. Szoka A., Gajowiec G., Zieliński A., Serbinski W., Olive J.-M., Ossowska A.: Hydrogen degradation of pre-oxidixed zirconium alloys, Adv. Mater. Sci. 17 (2017) 5–21.
6. Couet A., Motta A.T., Comstock R.J.: Hydrogen pickup measurements in zirconium alloys: Relation to oxidation kinetics, J. Nucl. Mater. 451 (2014) 1–13.
7. Fernández G.E., Meyer G., Peretti H.A.: Analysis of the hydride formation kinetics of Zry-4, J. Alloys Compd. 330–332 (2002) 483–487.

8. Kim Y.S., Ahn S.B., Cheong Y.M.: Precipitation of crack tip hydrides in zirconium alloys. J. Alloys Compd.. 429 (2007) 221–226.
9. Cox B.: Hydrogen uptake during oxidation of zirconium alloys. J. Alloys Compd. 256 (1997) 244–246.
10. Elmoselhi M.B.: Hydrogen uptake by oxidized zirconium alloys. J. Alloys Compd. 231 (1995) 716–721.
11. Khatamian D., Ling V.C.: Hydrogen solubility limits in α- and β-zirconium. J. Alloys Compd. 253–254 (1997) 162–166.
12. Chen W., Wang L., Lu S.: Influence of oxide layer on hydrogen desorption from zirconium hydride. J. Alloys Compd. 469 (2009) 142–145.
13. Yamanaka S., Nishizaki T., Uno M., Katsura M.: Hydrogen dissolution into zirconium oxide. J. Alloys Compd. 293 (1999) 38–41.
14. Allen T.R., Konings R.J.M., Motta A.T.: Corrosion of Zirconium Alloys, 1st ed., Elsevier Inc., 2012.
15. Khatamian D.: Solubility and partitioning of hydrogen in metastable Zr-based alloys used in the nuclear industry. J. Alloys Compd. 293 (1999) 893–899.
16. Cox B.: Hydrogen trapping by oxygen and dislocations in zirconium alloys. J. Alloys Compd. 256 (1997) L4–L7.
17. Giroldi J.P., Vizcaíno P., Flores A.V., Banchik A.D.: Hydrogen terminal solid solubility determinations in Zr-2.5Nb pressure tube microstructure in an extended concentration range. J. Alloys Compd. 474 (2009) 140–146.
18. Singh R.N., Mukherjee S., Gupta A., Banerjee S.: Terminal solid solubility of hydrogen in Zr-alloy pressure tube materials. J. Alloys Compd. 389 (2005) 102–112.
19. Roustila A., Chêne J., Séverac C.: XPS study of hydrogen and oxygen interactions on the surface of the NiZr intermetallic compound. Intl. J. Hydrogen Energy 32 (2007) 5026–5032.
20. Lee K.W., Hong S.I.: Zirconium hydrides and their effect on the circumferential mechanical properties of Zr-Sn-Fe-Nb tubes. J. Alloys Compd. 346 (2002) 302–307.
21. Steinbrück M., Bottcher M.: Air oxidation of Zircaloy-4, M5® and ZIRLO™ cladding alloys at high temperatures. J. Nucl. Mater. 414 (2011) 276–285.
22. Bertolino G., Meyer G., Perez Ipiña J., :n situ crack growth observation and fracture toughness measurement of hydrogen charged Zircaloy-4. J. Nucl. Mater. 322 (2003) 57–65.
23. Bertolino G., Meyer G., Perez Ipiña J.: Effects of hydrogen content and temperature on fracture toughness of Zircaloy-4. J. Nucl. Mater. 320 (2003) 272–279.
24. Bertolino G., Meyer G., Perez Ipia J.: Degradation of the mechanical properties of Zircaloy-4 due to hydrogen embrittlement. J. Alloys Compd. 330–332 (2002) 408–413.
25. Hong S.I., Lee K.W., Kim K.T.: Effect of the circumferential hydrides on the deformation and fracture of Zircaloy cladding tubes. J. Nucl. Mater. 303 (2002) 169–176.
26. Rajasekhara S., Kotula P.G., Enos D.G., Doyle B.L., Clark B.G.: Influence of Zircaloy cladding composition on hydride formation during aqueous hydrogen charging. J. Nucl. Mater. 489 (2017) 222-228.
27. Zieliński A., Cymann A., Guminski A., Szoka A., Gajowiec G.: Influence of high temperature oxidation on hydrogen absorption and degradation of Zircaloy-2 and Zr 700 alloys. High Temp. Mater. Techn. (2018), to be published.

28. Blackmur M.S., Robson J.D., Preuss M., Zanelatto O., Cernik R.J., Shi S.-Q., Ribeiro F., Andrieux J.: Zirconium hydride precipitation kinetics in Zircaloy-4 observed with synchrotron X-ray diffraction. J. Nucl. Mater. 464 (2015) 160-169.

29. Burr P.A., Murphy S.T., Lumley S.C., Wenman M.R., Grimes R.W.: Hydrogen solubility in zirconium intermetallic second phase particles. J. Nucl. Mater. 443 (2013) 502-506.